Rare Metal Materials and Engineering
Volume 53, Issue 6, June 2024
Available online at www.rmme.ac.cn

Science Press

Cite this article as: Wang Chunshui, Wu Haiyan, Jiao Cheng, et al. Gas Sensing Properties of $C_3N_4/CuGaO_2$ Composites Prepared by Hydrothermal Method[J]. Rare Metal Materials and Engineering, 2024, 53(06): 1536-1542. DOI: 10.12442/j.issn.1002-185X.E20230035.

ARTICLE

Gas Sensing Properties of $C_3N_4/CuGaO_2$ Composites Prepared by Hydrothermal Method

Wang Chunshui[1], **Wu Haiyan**[1], **Jiao Cheng**[1], **Chu Xiangfeng**[1], **Liang Shiming**[2], **He Lifang**[1]

[1] Anhui University of Technology, Ma'anshan 243002, China; [2] Linyi University, Linyi 276005, China

Abstract: A series of $C_3N_4/CuGaO_2$ composites were synthesized by facile hydrothermal method. The prepared samples were characterized by XRD, SEM, TEM, and XPS. The gas sensing properties of the $C_3N_4/CuGaO_2$ composites were investigated. Results demonstrate that the gas sensor based on $C_3N_4/CuGaO_2$-0.3 composite (molar ratio of C_3N_4 to $CuGaO_2$ is 0.3:1) shows better sensing performance to toluene than $CuGaO_2$ sensor does. Compared with the operating temperature of $CuGaO_2$ sensor (140 °C), the optimal working temperature of $C_3N_4/CuGaO_2$-0.3 composite sensor is only 25 °C, the response to 100 μL/L toluene gas reaches 28, and the detection limit is as low as 0.01 μL/L. The response time and recovery time for the detection of 100 μL/L toluene vapor are 114.2 and 27.4 s, respectively. Moreover, the $C_3N_4/CuGaO_2$-0.3 composite sensor also exhibits excellent long-term stability, good repeatability, and extraordinary humidity resistance for toluene detection.

Key words: C_3N_4; $CuGaO_2$; gas sensing; toluene

Toluene is one of the hazardous and harmful gases released from the process of room decoration and chemical production. Human may suffer from headache, dizziness, and even serious kidney damage due to toluene[1]. Although the exhaled gas also contains toluene, the toluene concentration of a healthy breathe is only 0.005 – 0.02 μL/L, and the toluene concentration of exhaled gas of lung cancer patients is 0.02 – 0.03 μL/L[2]. Therefore, the toluene concentration from human breath can be used as a critical indicator for the diagnosis of patients with lung cancer. It is of great significance to manufacture gas sensor for accurate toluene detection at μL/L level for lung cancer diagnosis.

In recent years, spinel-type oxides, such as $NiFe_2O_4$, $ZnFe_2O_4$, and $NiCa_2O_4$, have gained widespread interest due to their exceptional chemical properties and unique structures[3–4], and therefore the spinel-type oxide-based sensors for toluene detection have also been conducted. Chen et al[5] prepared $NiGa_2O_4$/NiO composite by solvothermal method, the response of the 50wt% $NiGa_2O_4$/NiO-based gas sensor to 100 μL/L toluene at 230 °C was 12.7, and the detection limit to toluene reached 0.5 μL/L. Hollow urchin-like core-shell spinel-structured $ZnFe_2O_4$ material was prepared via the solvothermal method. Results show the response of 79 to 100 μL/L toluene at the operating temperature of 250 °C, and the detection limit is 0.2 μL/L[6]. Moreover, $CuGaO_2$, as one of spinel-type oxides, attracts much attention due to its good stability and high hole mobility[7]. However, $CuGaO_2$ material is rarely used for toluene detection. The graphitic carbon nitride (C_3N_4) with band-gap of about 2.7 eV is a kind of two-dimensional semiconductor material, which has been widely studied for its good chemical stability, nontoxicity, large specific surface area, and low cost[8–10]. More importantly, its special layered structure is beneficial to the transport of electrons and oxygen molecules, which promotes the adsorption of target gas[11]. It is reported that an appropriate amount of g-C_3N_4 can effectively improve the gas sensing properties of metal oxides[12]. Zhang et al[13] prepared g-C_3N_4/α-Fe_2O_3 nanocomposites by hydrothermal method, and the response of 60wt% g-C_3N_4/α-Fe_2O_3-based gas sensor reached 7.76 to 100 μL/L ethanol, which was 1.8 times higher than that of pure α-Fe_2O_3. Wang et al[14] prepared the g-C_3N_4/WO_3 nanomaterials via liquid ultrasonic mixing method, the response of 1wt% g-C_3N_4/WO_3 composite-based gas sensor to 100 μL/L acetone was 35, which was 3 times higher than that of pure WO_3, and its response time and recovery time were 9.0 and 3.8 s, respectively. Therefore, it is reasonable to

---

Received date: September 13, 2023
Foundation item: National Natural Science Foundation of China (61971003); National Natural Science Foundation of Shandong Province (ZR2020MF025)

Corresponding author: Chu Xiangfeng, Ph. D., Professor, Anhui University of Technology, Ma'anshan 243002, P. R. China, E-mail: xfchu99@ahut.edu.cn

assume that the addition of C_3N_4 may improve the gas sensing performance of $CuGaO_2$ material.

In this research, a series of C_3N_4/$CuGaO_2$ composites with different C_3N_4 contents were synthesized by hydrothermal method and their gas sensing properties were studied. This research provided a new approach to prepare high-performance sensor for the detection of toluene gas.

1 Experiment

Melamine (5 g) was placed into a muffle furnace and calcined at 550 °C for 4 h with the heating rate of 2 °C/min. The yellow C_3N_4 powder was collected after the muffle furnace cooling to room temperature[15].

Firstly, 1.2 mmol $Cu(NO_3)_2 \cdot 3H_2O$, 1.2 mmol $Ga(NO_3)_3 \cdot 9H_2O$, and 0.25 g cetyltrimethylammonium bromide were dissolved in 30 mL deionized water through stirring to form the mixed solution. Then, 10 mL ethylene glycol was added into the mixed solution by magnetic stirring for 30 min. Afterwards, C_3N_4 was added into the mixed solution. The molar ratio of C_3N_4 to $CuGaO_2$ was 0:1, 0.1:1, 0.3:1, 0.5:1, 0.8:1, and 1.0:1. The mixture was sonicated for 6 h, and then 2 mol/L NaOH solution was slowly dripped to adjust the pH value of mixed suspension to 5.0. The suspension was transferred into 100 mL Teflon autoclave and kept at 190 °C for 12 h. The obtained product was washed by deionized water and ethanol for several times. Finally, the product was dried at 80 °C for 12 h in the oven. The powders were labeled as C-0, C-0.1, C-0.3, C-0.5, C-0.8, and C-1.0 based on the molar ratio of C_3N_4 to $CuGaO_2$ as 0: 1, 0.1: 1, 0.3: 1, 0.5: 1, 0.8: 1, and 1.0: 1, respectively.

The phase composition of the samples was analyzed by X-ray diffraction (XRD, Bruker D8 Advance, Cu Kα radiation, λ=0.154 18 nm, scanning rate of 10°/min). The sample morphologies were characterized by scanning electron microscope (SEM, Hitachi S-4800), transmission electron microscope (TEM, JM-2100), high resolution TEM (HRTEM), and fast-Fourier transform (FFT) analysis. X-ray photoelectron spectroscope (XPS, Thermo Scientific K-Alpha+model) was used to analyze the chemical state of the sample surface.

A small amount of gas sensing material was ground into mortar with two drops of terpineol, forming the paste. Then, it was evenly coated on the outside surface of Al_2O_3 ceramic tube (8 mm in length, 2 mm in inner diameter, and 2.6 mm in outer diameter) which was attached to gold electrodes and four Pt wires. The Ni-Cr heating coil was inserted into the ceramic tube to control the working temperature by adjusting the heating voltage, as shown in Fig. 1. Finally, the gas sensor was assembled and dried for 12 h in the oven. The sensor sensitivity S is defined as R_a/R_g, where R_a and R_g are the resistance of sensor in air and target gas, respectively. The response time is the time required for reaching 90% of the maximum sensitivity in response process. The recovery time is the time required for reaching 90% of the original resistance in the recovery process.

2 Results and Discussion

2.1 Characterization

Fig. 2 shows XRD patterns of pure C_3N_4 and C_3N_4/$CuGaO_2$ composites. The diffraction peaks of the as-prepared C-0 sample are consistent with the standard peaks of $CuGaO_2$ (PDF#41-0255), so it can be confirmed that the as-prepared C-0 sample is $CuGaO_2$. The diffraction peaks at 15.48°, 31.25°, 36.37°, 40.82°, 55.71°, 62.36°, 65.27°, 71.39°, and 74.38° correspond to (003), (006), (012), (104), (018), (110), (1010), (116), and (202) crystal planes of $CuGaO_2$, respectively[7]. The diffraction peak of C_3N_4/$CuGaO_2$ composites at 27.64° corresponds to the (002) crystal plane of C_3N_4. With the increase in C_3N_4 content, the diffraction peak intensity of C_3N_4 phase is significantly enhanced, indicating that the C_3N_4 content in the composite is increased[16]. The existence of the diffraction peaks of C_3N_4 and $CuGaO_2$ in C_3N_4/$CuGaO_2$ composites indicates the successful combination of C_3N_4 and $CuGaO_2$.

The microstructures of the as-prepared products were investigated by SEM and TEM. As shown in Fig. 3a, the $CuGaO_2$ material exhibits flower-like structure, which consists of many nanosheets. The flower-like structure can effectively increase the specific surface area of the material and improve the gas sensing properties of the composite materials[17]. According to Fig. 3b – 3f, with the increase in C_3N_4 content in the C_3N_4/$CuGaO_2$ composites, the flower-like morphology gradually disappears. Clearly, the morphology of C-1.0 sample is similar to that of the pure C_3N_4 sheet due to a large amount of C_3N_4 doped on the sample surface. Fig. 3g shows SEM image of the pure C_3N_4, which possesses multi-layer structure. As shown in Fig. 3h, it is clear that many small and irregular $CuGaO_2$ nanosheets are distributed on the C_3N_4 surface, illustrating the successful synthesis of the C-0.3 composite. Further, HRTEM image shows the lattice spacing of 0.340 and 0.283 nm, which corresponds to the (002) crystal plane of C_3N_4[10] and (006) crystal plane of $CuGaO_2$[7], respectively.

The chemical states and oxidation states of elements are

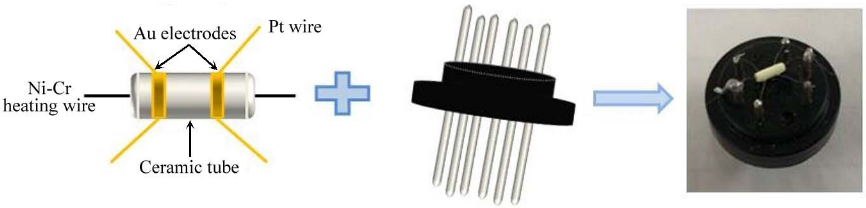

Fig.1 Schematic diagram of formation process of gas sensor device

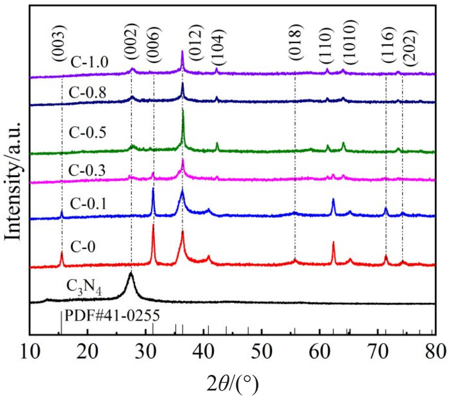

Fig.2 XRD patterns of pure C_3N_4, $CuGaO_2$, and $C_3N_4/CuGaO_2$ composites

analyzed by XPS. Fig.4a shows overall XPS spectra of C-0.3 composite sample, which confirms the presence of Cu, Ga, O, C, and N elements. Two peaks exist in the Cu 2p spectra, which are located at 932.2 and 952.0 eV, corresponding to Cu $2p_{3/2}$ and Cu $2p_{1/2}$, respectively. Further, the binding energy difference of 19.8 eV between Cu $2p_{3/2}$ and Cu $2p_{1/2}$ agrees well with the fact that all copper atoms exist as Cu^+ form[18–19]. XPS spectra of Ga 2p of C-0.3 sample have two peaks, which are located at 1117.6 and 1144.5 eV, corresponding to Ga $2p_{3/2}$ and Ga $2p_{1/2}$, respectively, as shown in Fig.4c. It can be seen that Ga^{3+} is located at the octahedral and tetrahedral sites. Additionally, the binding energy difference of 26.9 eV between Ga $2p_{3/2}$ and Ga $2p_{1/2}$ agrees well with the results in Ref.[20]. The N 1s spectra in Fig.4d show three peaks, which are located at 395.0, 397.0, and 399.0 eV, corresponding to the N-ring hybridized by sp^2 (C=N-C), the N-$(C)_3$ form, and the N element in the H-N structure, respectively. The C 1s peak (Fig.4e) can be divided into three peaks, which are located at 284.5, 285.0, and 287.9 eV, corresponding to C-C, C-N, and N-C=N, respectively[21]. The O 1s spectra in Fig.4f show three peaks, which are located at 530.0, 531.0, and 532.0 eV, corresponding to the surface lattice oxygen, surface adsorbed oxygen, and hydroxyl oxygen, respectively. Furthermore, the content of O_L, O_C, and O_V oxygen species in C-0.3 sample is shown in Table 1. The amount of oxygen adsorbed on the surface significantly influences the gas sensing properties of the gas sensor[22].

Fig. 5 shows the nitrogen adsorption-desorption isotherms and pore size distributions of C-0 and C-0.3 samples. According to IUPAC classification, the physisorption

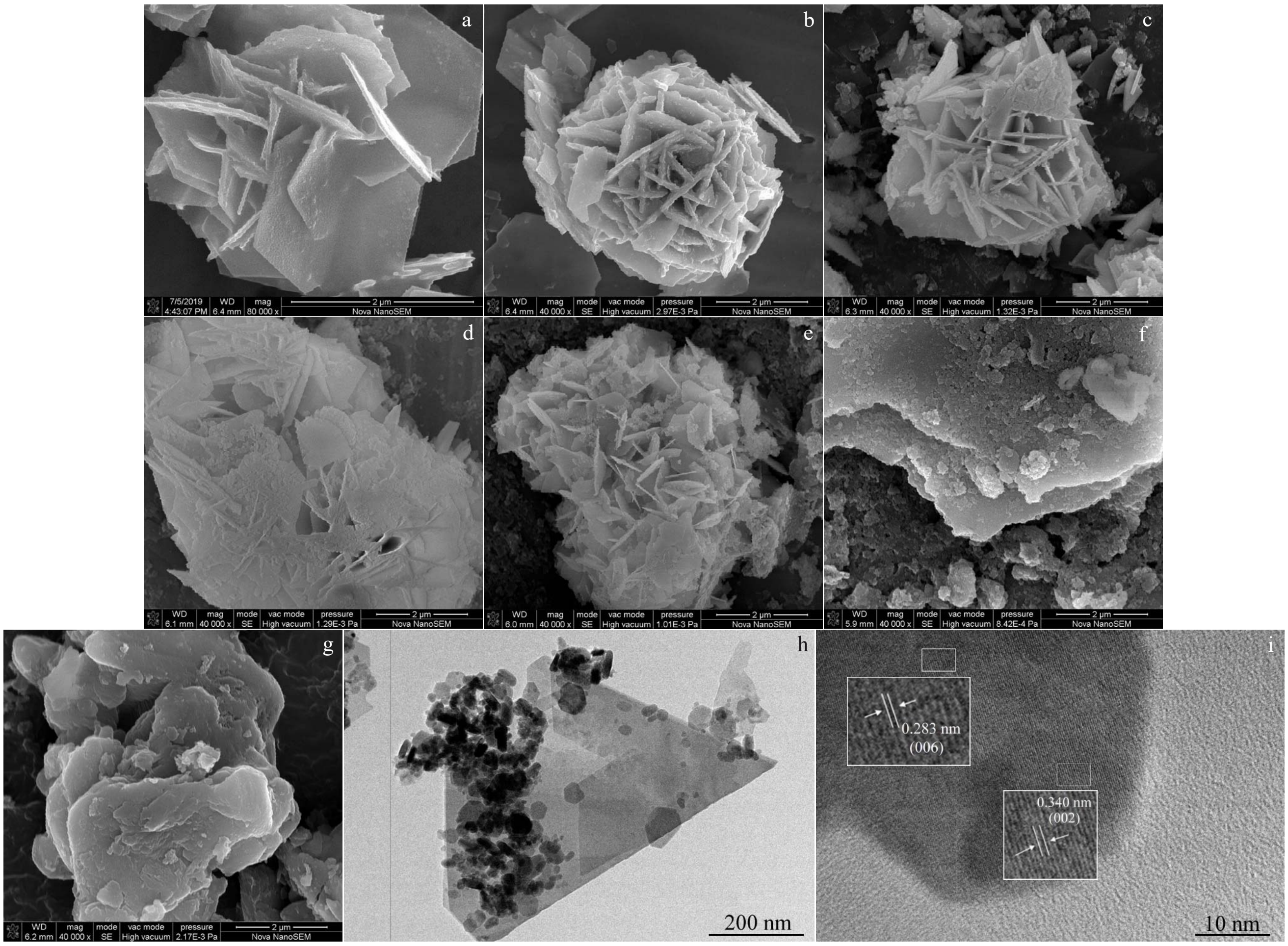

Fig.3 SEM images of C-0 (a), C-0.1 (b), C-0.3 (c), C-0.5 (d), C-0.8 (e), C-1.0 (f) samples, and pure C_3N_4 (g); TEM image (h) and HRTEM image with FFT patterns (i) of C-0.3 sample

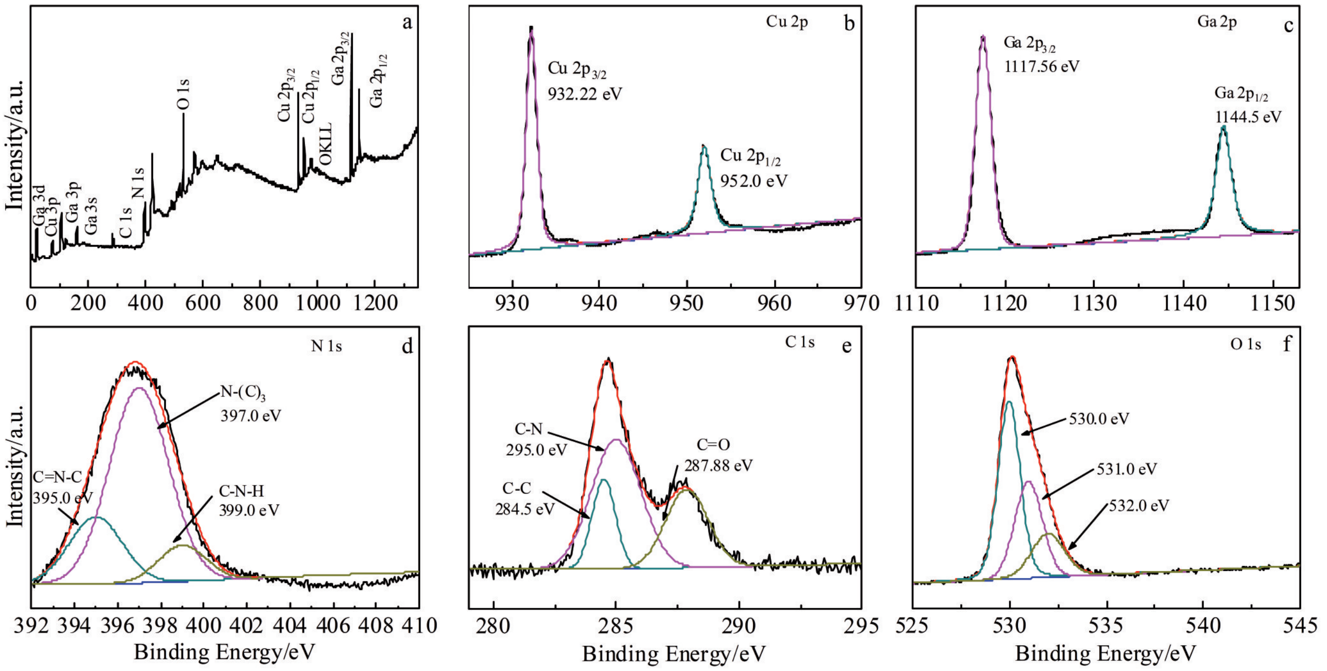

Fig.4 XPS spectra of C-0.3 sample: (a) overall; (b) Cu 2p; (c) Ga 2p; (d) N 1s; (e) C 1s; (f) O 1s

Table 1 XPS peak area ratios of different oxygen species in C-0.3 sample

Sample	Oxygen species	Peak area ratio/%
C-0.3	O_L	43.8
	O_C	34.5
	O_V	21.7

isotherms and hysteresis loops of C-0 and C-0.3 samples belong to the IV type and H3 type, respectively, which indicates that mesoporous structures exist in the samples[23]. Besides, the pore diameters of C-0 and C-0.3 samples are mainly concentrated at 3.0 and 10 nm, respectively. As shown in Table 2, the BET specific surface areas of C-0, C-0.1, C-0.3, C-0.5, C-0.8, and C-1.0 samples are 1.77, 5.97, 20.06, 28.50, 36.09, and 44.14 m^2/g, respectively. The addition of C_3N_4 significantly increases the specific surface area of $CuGaO_2$ material, therefore enhancing the gas adsorption and improving the gas sensing properties[24].

2.2 Gas sensing properties

Fig. 6a reveals the response of gas sensors based on C_3N_4/$CuGaO_2$ samples to acetone, ethanol, acetic acid, toluene, trimethylamine, ammonia, and methanol of 100 μL/L. It can be seen that C-0.3 composite-based gas sensor shows the highest response and excellent selectivity to toluene at 25 °C. The response of C-0.3 sample to toluene of 100 μL/L is 28, whereas that to other gases is lower than 15, suggesting its outstanding selectivity for toluene detection. To assess the selectivity of gas sensors based on pristine $CuGaO_2$ and C-0.3 sample, their response to toluene was tested at different temperatures. As shown in Fig. 6b, C-0.3 composite-based sensor shows high sensitivity to toluene at any temperature. Further, the C-0.3 composite-based sensor has the highest response at room temperature (25 °C), which indicates that the optimal operating temperature of the C-0.3 composite-based sensor is 25 °C. On the contrary, the pristine $CuGaO_2$-based sensor presents relatively low response at every temperature, illustrating poor selectivity. Therefore, it can be concluded that C_3N_4 is beneficial to decrease the optimal working temperature and improve the gas sensing properties.

The dynamic sensing transients of sensors based on C-0.3 composite for toluene detection at 25 °C are shown in Fig. 7a. With the increase in toluene content, the response of C-0.3 composite-based sensor to toluene is also increased. The response of C-0.3 composite-based sensor to toluene of 100, 80, 50, 10, 1, 0.1, and 0.01 μL/L is 28.00, 22.59, 16.23, 10.17, 3.18, 1.92, and 1.14, respectively. This suggests that the detection limit of sensor is 0.01 μL/L. Besides, the response and recovery time are also important parameters for gas sensors. As shown in Fig. 7b, it is clear that the response time and recovery time for toluene of 100 μL/L are about 114.2 and 27.4 s, respectively, indicating the fast detection speed of the sensor. To investigate the reproducibility of C-0.3 composite-based sensor, four cycles of dynamic response-recovery tests were conducted, and the results are shown in Fig. 7c. The response of four cycles is 29.6, 27.8, 30.5, and 27.9, presenting a relatively low deviation. It can be seen that the adsorption-desorption phenomenon of C-0.3 composite to toluene is reversible and it has good reproducibility[25]. Fig. 7d shows the linear calibration relationship between the response and toluene content. It can be seen that the correlation can be evaluated by R^2 (R^2=0.9544), and the sensor is sensitive to the toluene with low content.

The influence of humidity and the long-time stability on gas sensing performance is important for the practical application. As shown in Fig. 8a, with the increase in relative humidity

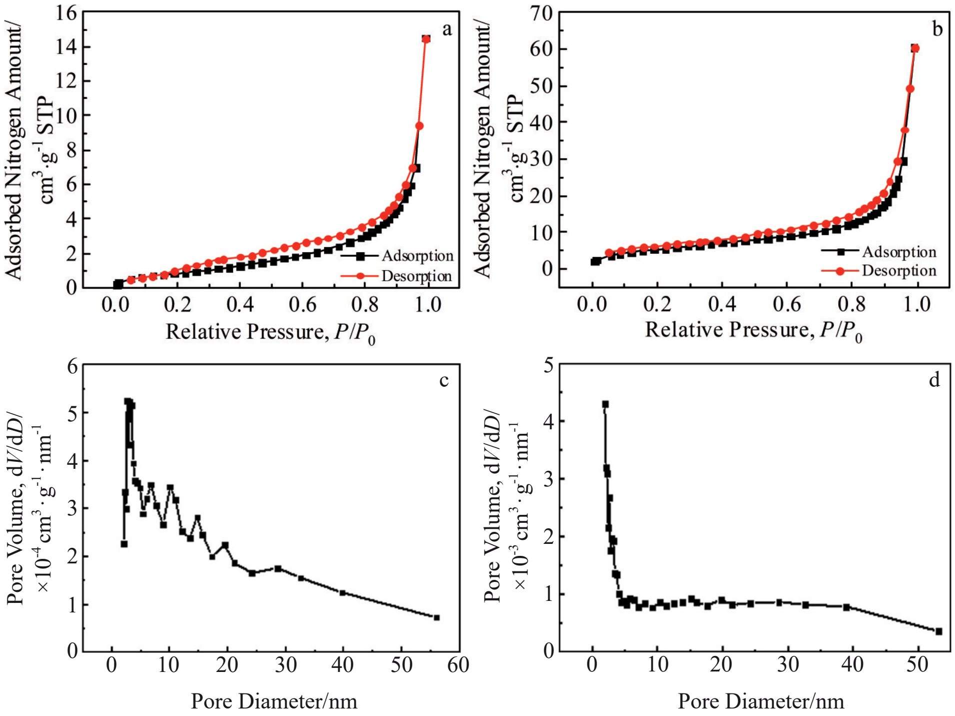

Fig.5 Nitrogen adsorption-desorption isotherms (a–b) and pore size distributions (c–d) of C-0 (a, c) and C-0.3 (b, d) samples

Table 2 BET specific surface area of pure C_3N_4 and C_3N_4/$CuGaO_2$ samples (m^2/g)

Sample	C-0	C-0.1	C-0.3	C-0.5	C-0.8	C-1.0
BET specific surface area	3.33	5.97	20.06	28.50	36.09	44.14

from 20% to 60%, the response of the C-0.3 composite-based sensor is relatively stable. However, when the relative humidity exceeds 60%, the response of C-0.3 composite-based sensor significantly decreases. This can be explained by the fact that H_2O molecules compete with the O_2 molecules to trap the electrons form the C-0.3 sample, thereby promoting the elimination of active sites[26]. Besides, the poor response to toluene of 0 µL/L indicates that this material is insensitive to H_2O molecules, reflecting the superb moisture resistance. Fig.8b shows the long-term stability of C-0.3 composite-based sensor, and it can be used continuously for 15 d. The response to toluene of 100 µL/L has no obvious fluctuation, confirming its good stability.

2.3 Gas sensing mechanism

The gas sensing mechanism of C_3N_4/$CuGaO_2$ composites is associated with the change in electrical conductivity, according to the adsorption/desorption of target gas and oxygen molecules[27]. It is known that O_2 molecules can capture the electrons from oxide semiconductors to form O_2^- species below 100 °C[28]. As shown in Fig.9, when the C_3N_4/$CuGaO_2$ composites are placed in air, due to the adsorption effect of material, the adsorbed oxygen molecules may trap the electrons to form various oxygen species. After equilibrium, the electrical resistance of $CuGaO_2$ material increases. After exposure to toluene, the toluene reacts with oxygen ions adsorbed on the material surface, and the obtained electrons will be released back to conduction band,

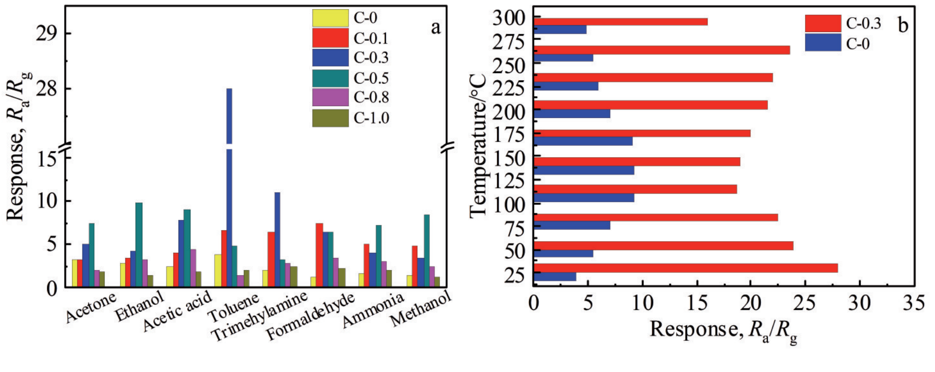

Fig.6 Response of C_3N_4/$CuGaO_2$ samples to different gases of 100 µL/L at 25 °C (a); response of gas sensors based on C-0 and C-0.3 samples to toluene of 100 µL/L at different temperatures

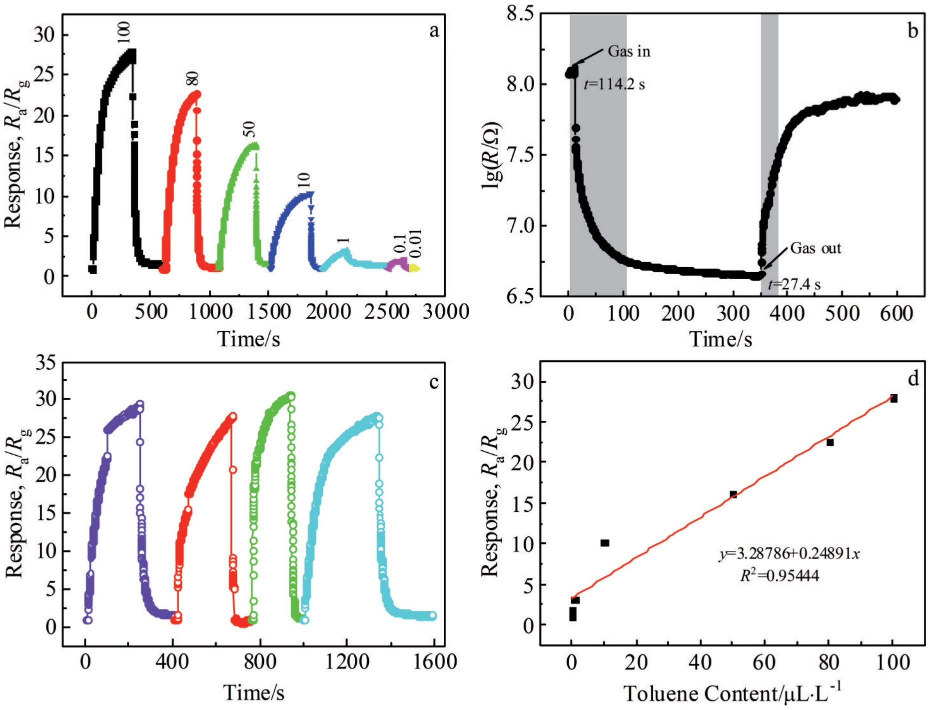

Fig.7 Sensing properties of C-0.3 composite-based sensor to toluene at 25 °C: (a) response-recovery curves; (b) dynamic response curves; (c) reproducibility curve; (d) linear relationship of response

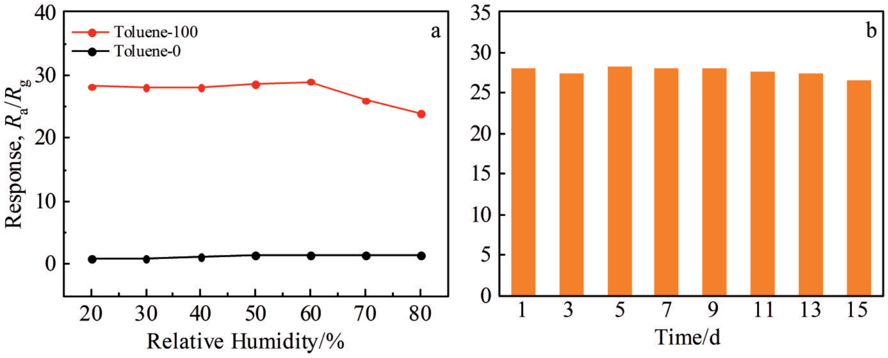

Fig.8 Response of C-0.3 composite-based sensor at different relative humidity at 25 °C (a); repeated sensing stability of C-0.3 composite-based sensor to toluene of 100 μL/L at 25 °C (b)

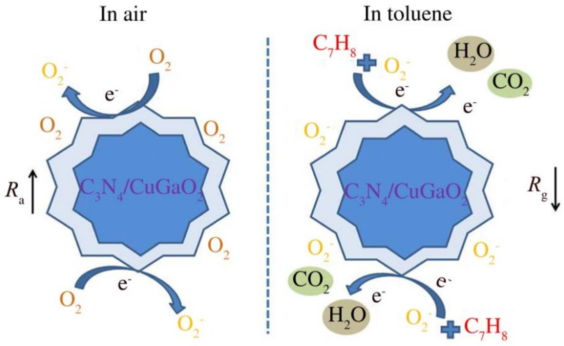

Fig.9 Sensing mechanism of C_3N_4/CuGaO$_2$ composite

which results in the decrease in electrical resistance of the sensor device[29]. The reaction equations are as follows:

$$O_2\,(gas) \rightarrow O_2\,(ads) \tag{1}$$

$$O_2\,(ads)+e^- \rightarrow O_2^-(ads) \quad <100\ °C \tag{2}$$

$$C_7H_8\,(gas)+9O_2^-\,(ads) \rightarrow 7CO_2\,(gas)+4H_2O\,(gas)+9e^- \tag{3}$$

3 Conclusions

1) The enhanced sensing property of CuGaO$_2$ is caused by the addition of C_3N_4, which can improve the response and gas sensing selectivity.

2) The C-0.3 composite-based sensor has high response to toluene of 100 μL/L at the operating temperature of 25 °C. The detection limit is 0.01 μL/L, and the gas sensing selectivity to toluene is excellent. This research offers a promising sensor to detect toluene at room temperature with high response and good long-time stability.

References

1 Hermawan A, Asakura Y, Inada M *et al. Ceramics International*[J], 2019, 45(12): 15435

2 Gregis G, Sanchez J B, Bezverkhyy I *et al. Sensors and Actuators B: Chemical*[J], 2018, 255: 391

3 Zhang Y L, Zhou Y, Li Z L *et al. Journal of Alloys and Compounds*[J], 2019, 784: 102

4 Jiang L, Xue K, Chen Z *et al. Materials Science in Semiconductor Processing*[J], 2021, 134: 106051

5 Chen H, Ao S, Li G D *et al. Sensors and Actuators B: Chemical*[J], 2019, 282: 331

6 Zhang H, Hu J H, Li M W *et al. Sensors and Actuators B: Chemical*[J], 2021, 349: 130734

7 Choi M U, Hayakawa T. *Materials Research Bulletin*[J], 2019, 113: 84

8 Lafta M, Ammar S. *Materials Science in Semiconductor Processing*[J], 2023, 153: 107131

9 Yang Y, Ji T, Yang Z *et al. Construction and Building Materials*[J], 2020, 234: 117438

10 Zhang H, Ouyang T W, Li J M *et al. Electrochimica Acta*[J], 2021, 390: 138766

11 Zhou D F, Qiu C Q. *Chemical Physics Letters*[J], 2019, 728: 70

12 Koli P, Birari M, Ahire S *et al. Inorganic Chemistry Communications*[J], 2022, 146: 110083

13 Zhang Y J, Zhang D K, Guo W M *et al. Journal of Alloys and Compounds*[J], 2016, 685: 84

14 Wang D, Huang S M, Li H J *et al. Sensors and Actuators B: Chemical*[J], 2019, 282: 961

15 Zhong Q D, Lan H Y, Zhang M M *et al. Ceramics International*[J], 2020, 46(8B): 12192

16 Alhanash A, Al-Namshah K, Mohamed K *et al. Optik*[J], 2019, 186: 34

17 Xu W, Qiu C J, Zhou J *et al. Ceramics International*[J], 2020, 46(8A): 11372

18 Manickam R, Biswas K. *Journal of Alloys and Compounds*[J], 2019, 775: 1052

19 Xiong D H, Chang H M, Zhang Q Q *et al. Applied Surface Science*[J], 2015, 347: 747

20 Chu X F, Wang J L, Bai L S *et al. Materials Science and Engineering B*[J], 2018, 228: 45

21 Kumar A, Singh S, Khanuja M. *Materials Chemistry and Physics*[J], 2020, 243: 122402

22 Daichakomphu N, Sakdanuphab R, Harnwunggmoung A *et al. Solid State Ionics*[J], 2018, 328: 17

23 Akhtar A, Sadaf S, Liu J *et al. Journal of Alloys and Compounds*[J], 2022, 911: 165048

24 Guo W W, Huang L L, Zhang J *et al. Sensors and Actuators B: Chemical*[J], 2021, 334: 129666

25 Devi G S, Reddy P P S, Ramya K. *Materials Today: Proceedings*[J], 2016, 3(2): 224

26 Yin M L, Zhu Z. *Journal of Alloys and Compounds*[J], 2019, 789: 941

27 Miller D, Akbar S, Morris P. *Sensors and Actuators B: Chemical*[J], 2014, 204: 250

28 Ganesh R, Navaneethan M, Patil V *et al. Sensors and Actuators B: Chemical*[J], 2018, 255: 672

29 Seekaew Y, Wisitsoraat A, Phokharatkul D *et al. Sensors and Actuators B: Chemical*[J], 2019, 279: 69

水热法制备$C_3N_4/CuGaO_2$复合物及其气敏性能

王春水[1]，吴海燕[1]，焦　成[1]，储向峰[1]，梁士明[2]，何丽芳[1]

(1. 安徽工业大学，安徽 马鞍山 243002)

(2. 临沂大学，山东 临沂 276005)

摘　要：采用简单水热法合成了一系列$C_3N_4/CuGaO_2$复合材料。采用XRD、SEM、TEM和XPS对制备的样品进行了表征。研究了一系列$C_3N_4/CuGaO_2$复合材料的气敏性能。结果表明，基于$C_3N_4/CuGaO_2$-0.3复合材料（C_3N_4与$CuGaO_2$的摩尔比为0.3:1）的气体传感器对甲苯的传感性能优于$CuGaO_2$传感器。相比较于$CuGaO_2$传感器的工作温度（140 ℃），$C_3N_4/CuGaO_2$-0.3复合材料传感器的最佳工作温度仅为25 ℃，对100 μL/L甲苯气体的响应达到28，检出限低至0.01 μL/L。对100 μL/L甲苯气体的响应时间和恢复时间分别为114.2和27.4 s。此外，用于检测甲苯的$C_3N_4/CuGaO_2$-0.3复合材料传感器还具有优异的长期稳定性、良好的重复性和优异的抗湿性能。

关键词：C_3N_4；$CuGaO_2$；气体传感器；甲苯

作者简介：王春水，女，1999年生，硕士生，安徽工业大学，安徽 马鞍山 243002，E-mail：wcs1638375331@163.com